



HAL
open science

Microplasticity in polycrystalline pure copper subjected to very high cycle fatigue: thermal and microstructural analyses

Ngoc-Lam Phung, Antoine Blanche, Nicolas Ranc, André Chrysochoos, Véronique Favier

► To cite this version:

Ngoc-Lam Phung, Antoine Blanche, Nicolas Ranc, André Chrysochoos, Véronique Favier. Microplasticity in polycrystalline pure copper subjected to very high cycle fatigue: thermal and microstructural analyses. Colloque SF2M, 2011, Paris, France. 8 p. hal-00858940

HAL Id: hal-00858940

<https://hal.science/hal-00858940>

Submitted on 6 Sep 2013

HAL is a multi-disciplinary open access archive for the deposit and dissemination of scientific research documents, whether they are published or not. The documents may come from teaching and research institutions in France or abroad, or from public or private research centers.

L'archive ouverte pluridisciplinaire **HAL**, est destinée au dépôt et à la diffusion de documents scientifiques de niveau recherche, publiés ou non, émanant des établissements d'enseignement et de recherche français ou étrangers, des laboratoires publics ou privés.

Microplasticity in polycrystalline pure copper subjected to very high cycle fatigue: thermal and microstructural analyses

NGOC-LAM PHUNG^a, ANTOINE BLANCHE^b, NICOLAS RANC^a, ANDRE CHRYSOCHOOS^b, VERONIQUE FAVIER^a

^aArts et Métiers ParisTech, PIMM UMR CNRS 8006, 151 Boulevard de l'Hôpital, 75013 Paris, France

^bUniversité de Montpellier, LMGC UMR CNRS 5508 Université Montpellier II, Pl. E. Bataillon, 34095 Montpellier, France

Résumé: When ductile single-phase metallic materials are subjected to stress magnitudes lower than the conventional fatigue limit, the number of cycles to failure is higher than 10^9 , the so-called very high cycle fatigue (VHCF) regime. This work aims at studying the mechanism leading to crack initiation. The main challenge of this work results from the fact that the manifestations of the mechanisms of interest give rise to very low and localized signal owing to the very low stress magnitudes involved. To rapidly reach the VHCF regime, the ultrasonic fatigue technique has been used with the hourglass shaped plate specimen in commercial CuOF 99.95% copper. Using infrared thermography techniques, the temperature field at the specimen surface was measured during the fatigue test up to 10^8 cycles. Then, the dissipation in the variable section part of the specimen was calculated using a diffusion model. Moreover, the other surface was observed using a Scanning Electron Microscope (SEM) after interrupted tests at 10^6 , 10^7 and 10^8 cycles, respectively. At stress lower than 35 MPa, we did not observe any change of the specimen surface despite a significant self-heating induced by dissipation, whatever the number of cycles. For stress higher than 35 MPa, localized slip band appeared on the specimen surface and high dissipation zones were detected. The dissipation was found to increase higher and faster with increasing applied stress. The amount of slip bands observed on the specimen surface followed the same trend. In addition, two types of slip bands were observed: straight, concentrated, intensive slip bands and fine, spreading slip bands. These results suggested different plasticity behaviors of material which were correlated to the work of Stanzl-Tschegg and Schönbauer [9] who determined VHCF Persistent Slip Bands threshold at 45 MPa.

1 INTRODUCTION

The material could fail at stress amplitude well below the conventional fatigue limit. In these loading conditions, the number of cycles to failure could reach up to 10^9 cycles and belongs to the so-called very high cycle fatigue (VHCF) range. For materials of type I [1] as ductile single-phase fcc metals such as copper,

nickel, the fatigue failure initiates at the specimen surface. In High Cycle Fatigue (HCF) range, many studies confirmed the important role of Persistent Slip Bands (PSBs) in fatigue life of ductile fcc metals. At the free surface, PSBs appear as extrusions and intrusions with increasing cyclic number. These extrusions □ intrusions become more and more pronounced because of the accumulations of irreversible slips. This phenomenon promotes crack initiation at the surface of specimen and the fatigue failure. The aim of this study is to characterize the response of pure polycrystalline copper subjected to fatigue loading at stress amplitude below the conventional PSB threshold and after very high numbers of cycles. Following previous approaches focusing on high cycle fatigue range, we aim at analyzing slip markings appearing at the surface specimen and at relating them to the intrinsic dissipative response of the material in the VHCF response. Section 2 explains the experimental procedure and the method developed to determine the intrinsic dissipation from infrared red thermography measurements. Then, the evolutions of the intrinsic dissipation versus the number of cycles and the stress amplitudes related with the specimen surface changes are given in Section 3 and discussed in Section 4.

2 EXPERIMENTAL PROCEDURE AND DETERMINATION OF INTRINSIC DISSIPATION

Fatigue test

To reach VHCF regime within a reasonable time, ultrasonic fatigue technique at a testing frequency of about 20 kHz has been used at very small stress amplitude (lower than the VHCF fatigue limit of 92.2 MPa from [2]). Assuming an elastic behavior, the strain ratio, (minimum strain over maximum strain) was $R = -1$. One side of specimen was painted in black so that the heating change during loading will be captured by an infrared camera. From these temperature measurements, the intrinsic dissipation was determined using a 1D thermal model (see below). The fatigue experiments were periodically interrupted after prescribed numbers of loading so that the development of plastic slip markings on the other side surface was observed by optical and electronic microscopy.

Material

Ultrasonic fatigue hourglass shaped plate specimens in commercial polycrystalline copper CuOF 99.95% (supplied by Griset) were tested. The specimen dimension was determined so that the resonance frequency in tension-compression mode was 20 kHz. The dynamic Young modulus used for the design was $E_d = 130$ GPa [2]. A screw was soldered to the specimen to attach the specimen to the ultrasonic transducer. All specimens were treated at 250°C during 60 minutes to relieve the residual stress in the bulk specimen (ASM specialty Hand book). The resulting mean grain size was approximately 50 μm . After mechanical and electrolytic polishing, the specimen surfaces were mirror finish without any residual stresses. The geometry and the stress distribution along the specimen axis (calculated numerically) are presented in Figure 1; the

stress is theoretically concentrated in the middle of the gauge part of the specimen and reduced toward the specimen ends.

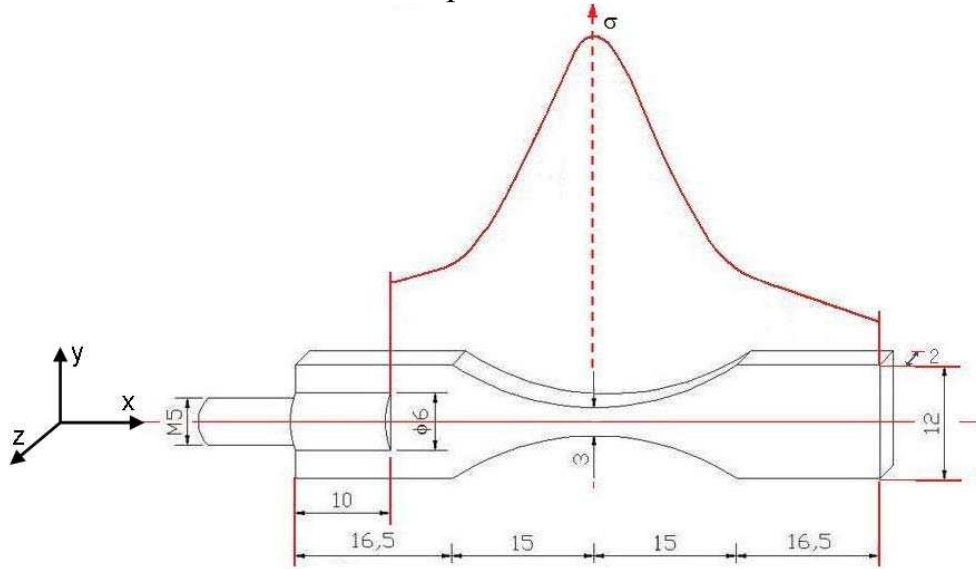


Figure 1. Ultrasonic fatigue plate specimen and distribution of stress range along the specimen axis.

Model of heat diffusion

A numerical model was built to estimate the distribution time course of intrinsic dissipation from temperature measurement fields during the fatigue test. We focused on the longitudinal distribution of heat sources within the specimen gauge part. A 1D calorimetric analysis has been justified assuming in a first approximation a uniaxial tension-compression stress state. From the heat equation:

$$\rho C \dot{T} - k \Delta T = s \quad (1)$$

where T is the temperature, ρ the mass density; C the heat capacity; k the thermal conduction coefficient. $s(x,y,z,t)$ symbolizes the volume of heat source. Following Boulanger's hypotheses [3], the 1D diffusion equation for a non-constant cross-section can be written as [4]:

$$\frac{\partial \theta(x,t)}{\partial t} + \frac{\theta(x,t)}{\tau^{1D}(x)} - \frac{k}{\rho C} \left(\frac{\partial^2 \theta(x,t)}{\partial x^2} + \frac{\partial \theta(x,t)}{\partial x} \frac{S'(x)}{S(x)} \right) = \frac{s(x,t)}{\rho C} \quad (2)$$

with $\theta = T - T^\circ$ is the temperature change, T° is the room temperature and τ^{1D} is a time constant term which characterizes the heat losses through lateral surfaces of the specimen:

$$\tau^{1D}(x) = \frac{\rho C \cdot S(x)}{2h(e+l(x))} \quad (3)$$

where e is the specimen thickness, $l(x)$ is its width with respect to x . We note $S(x) = e \cdot l(x)$ the cross-section at this point. The mean dissipation over several thousand cycles was solely estimated (the thermo elastic sources being not

considered here regarding the test frequencies and the adiabatic character of the thermoelastic processes over a complete cycle duration (50 μ s)). In the above equations, the unknown parameter is the heat transfer coefficient h . The method used to identify h is presented in the following section.

Heat loss time constant identification

The heat transfer coefficient is determined for each test, from thermal field measurements when the fatigue loading is stopped and the temperature of specimen returns to thermal equilibrium. More precisely, the initial temperature was considered as the temperature when the load was stopped. During the thermal return to equilibrium, no heat source occurs. Thermal measurements θ^{exp} applied to each end of the specimen by Dirichlet method enabled us to know the boundary conditions. The unknown heat transfer coefficient h was well chosen to satisfy these conditions:

$$\left\{ \begin{array}{l} \frac{\partial \theta(x,t)}{\partial t} + \frac{\theta(x,t)}{\tau^{1D}(x)} - \frac{k}{\rho C} \left(\frac{\partial^2 \theta(x,t)}{\partial x^2} + \frac{\partial \theta(x,t)}{\partial x} \frac{S'(x)}{S(x)} \right) = 0 \\ \theta(x,t=0) = \theta^{\text{exp}}(x,t=0) \\ \theta\left(\frac{-L}{2}, t\right) = \theta^{\text{exp}}\left(\frac{-L}{2}, t\right) \end{array} \right. \quad (4)$$

As a result, h was found in ranges of 30 \square 100 W/m²/K. This result shows that the heat losses are caused by natural convection and also by an air flow above the specimen which aims at cooling the piezoelectric system.

Dissipation calculation

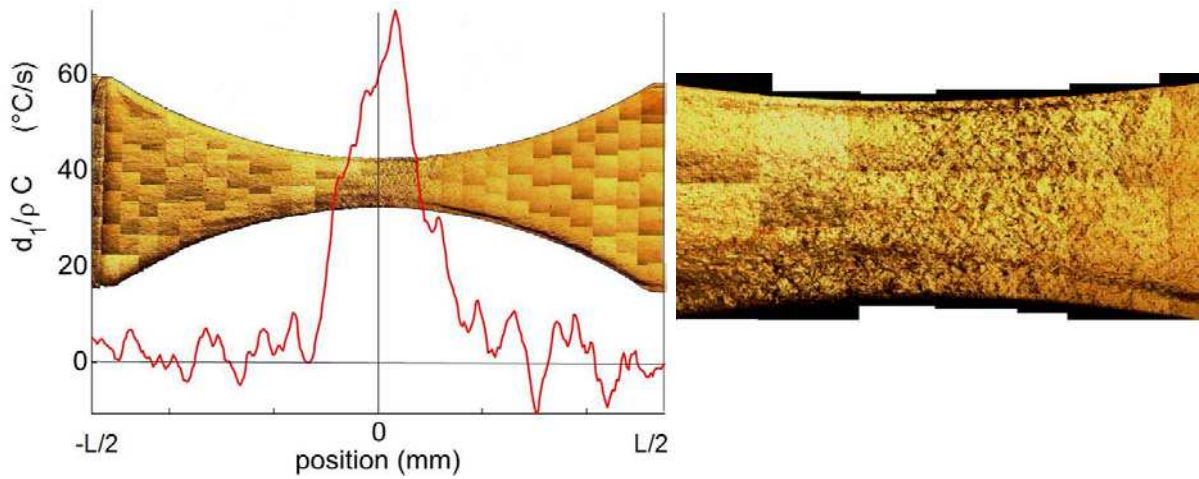
Once the heat transfer coefficient h is identified, it is possible to estimate the intrinsic dissipation d_I . The challenge is to solve the partial derivatives operators $\partial/\partial t$, $\partial/\partial x$ and $\partial^2/\partial x^2$ on the measured temperature which is a discrete and rough signal. A local \square least square \square fitting inspired by [3] was applied to approximate the temperature by an approximation function (5)

$$\theta^{\text{app}} = P_1 t x^2 + P_2 t x + P_3 t + P_4 x^2 + P_5 x + P_6 \quad (5)$$

3 RESULTS

Long-term fatigue test at constant maximum stress amplitude

Figure 2 shows the intrinsic dissipation distribution along the specimen axis obtained for maximal stress amplitude of 72.1 MPa after 10^7 cycles. The intrinsic dissipation is concentrated in the middle of the gauge specimen and decreases toward the ends. Hence, it is, as expected, related to the distribution of stress (Fig.1). Optical micrographs revealed that this zone displays the highest quantity of slip markings (Fig. 2). This result indicates that dissipation is related to microplasticity. In order to analyze the surface changes during cyclic loading, tests were interrupted after 10^6 , 10^7 , 10^8 cycles for various stress amplitudes.



(a)

(b)

Figure 2. Intrinsic dissipation along the specimen at $\Delta\sigma/2 = 72.1$ MPa, 10^7 cycles (a) and a zoom at the middle of gauge specimen (b)

Figure 3a and Figure 3b display the average temperature over the gauge length and over several thousands of cycles and the corresponding intrinsic dissipation for various maximum stress amplitudes versus the number of cycles. The temperature rises along the cycles and never reaches a constant value. In other words, the temperature does not stabilize, showing an evolution of the heat balance and consequently of the microstructure. Despite a slight raise of the temperature at $\Delta\sigma/2 = 45.9$ MPa, the intrinsic dissipation increased very slowly with the number of cycles was recorded. It reached up to 0.498 °C/s at 10^6 cycles and 0.505 °C/s at 10^8 cycles. It means that the heat sources were higher than the heat losses and remained active along the cycles. However, no slip bands were observed on specimen surface up to 10^8 cycles at this stress range. At $\Delta\sigma/2 = 51.5$ MPa, the intrinsic dissipation increased slowly up to 10^7 cycles. No slip bands were either observed between 10^6 and 10^7 cycles. At 10^8 cycles, a clear increase of the intrinsic dissipation was recorded. In this case, slip markings were also observed on the specimen surface, the intrinsic dissipation was 1.322 °C/s. These slip markings are very fine and straight and concentrated in cluster having low roughness (Fig. 4a). At higher stress amplitude, $\Delta\sigma/2 = 56.8$ MPa, the intrinsic dissipation increases with the number of cycles more rapidly than in previous cases. Slip bands were observed at 10^7 cycles, the intrinsic dissipation at this point was 1.412 °C/s. They were straight, isolated and highly rough, mainly located near the grain boundaries. The slip bands became progressively longer, rougher during cycling. In addition, some new parallel slip bands appeared close to the first ones (Fig. 4b and 4c). At $\Delta\sigma/2 = 72.1$ MPa, the intrinsic dissipation rises very fast with the number of cycles and reach to 7.477 °C/s at 10^6 cycles. Accordingly, some straight and rough slip bands were observed (Fig. 4d). At 10^7 cycles, the specimen surface at the middle part was entirely covered with slip bands (Fig 4e) so that the roughness

of specimen surface is obvious to the naked eyes. Note that all the slip markings are oriented at around $\pm 45^\circ$ from the loading direction.

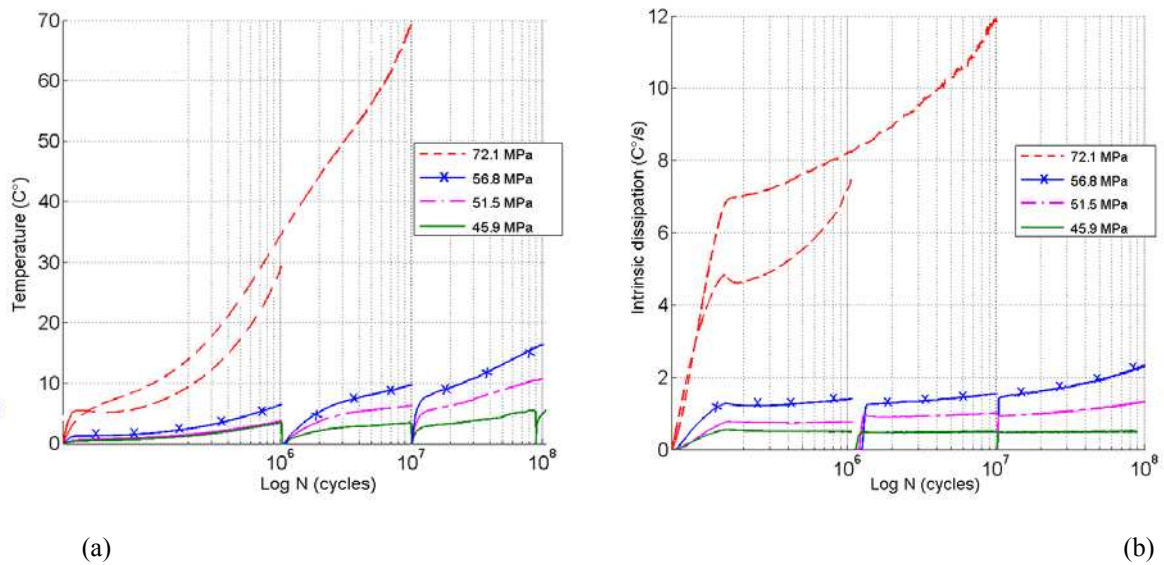


Figure 3. (a) Average temperature and (b) Average intrinsic dissipation during fatigue test at different constant stress amplitude fatigue test.

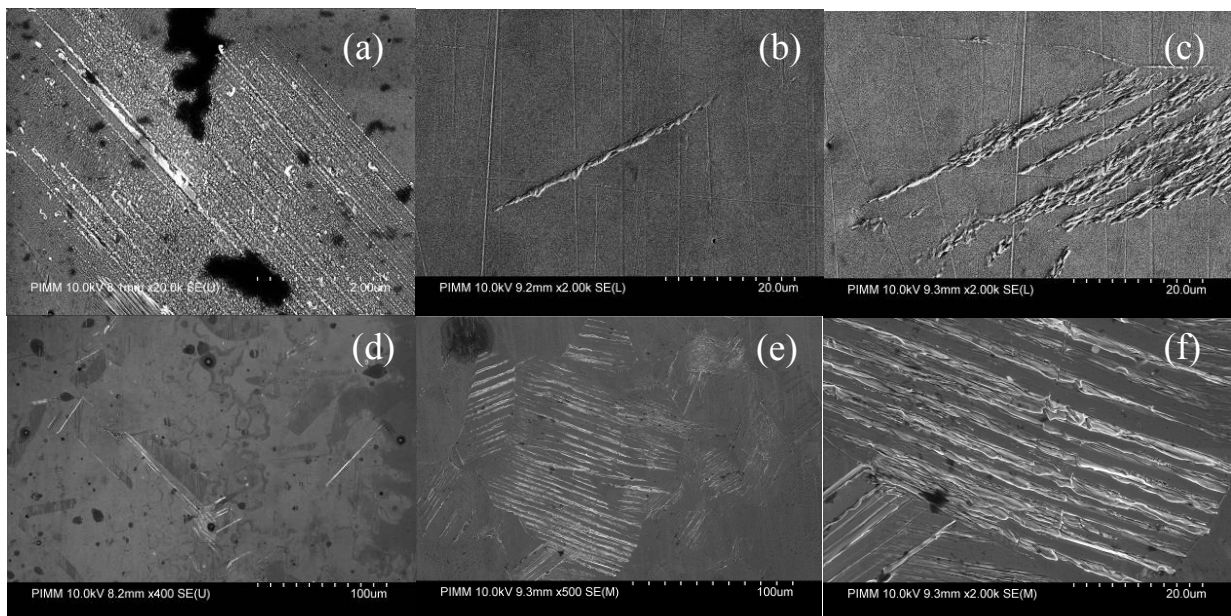


Figure 4. SEM micrographs of specimen surface at (a) $\Delta\sigma/2 = 51.5$ MPa after 10^8 ; at $\Delta\sigma/2 = 56.8$ MPa (b) after 10^7 cycles and (c) the same position after 10^8 cycles; at (d) $\Delta\sigma/2 = 72.1$ MPa after 10^6 cycles (e) $\Delta\sigma/2 = 72.1$ MPa after 10^7 cycles (f) a magnification of (d)

Intrinsic dissipation versus stress amplitude

Figure 5 shows the evolution of the average dissipation over the gauge length versus maximum stress amplitude at 10^7 cycles. Each dot corresponds to one cyclic loading test. The dissipation is found to slightly increase up to about 35 MPa. Then, the rise is steeper for higher stress amplitudes. These results

show the existence of a change of dissipative regime. This kind of result was mentioned by other works for high cycle fatigue regime [5-6] and was used for rapid determination of fatigue limit [7].

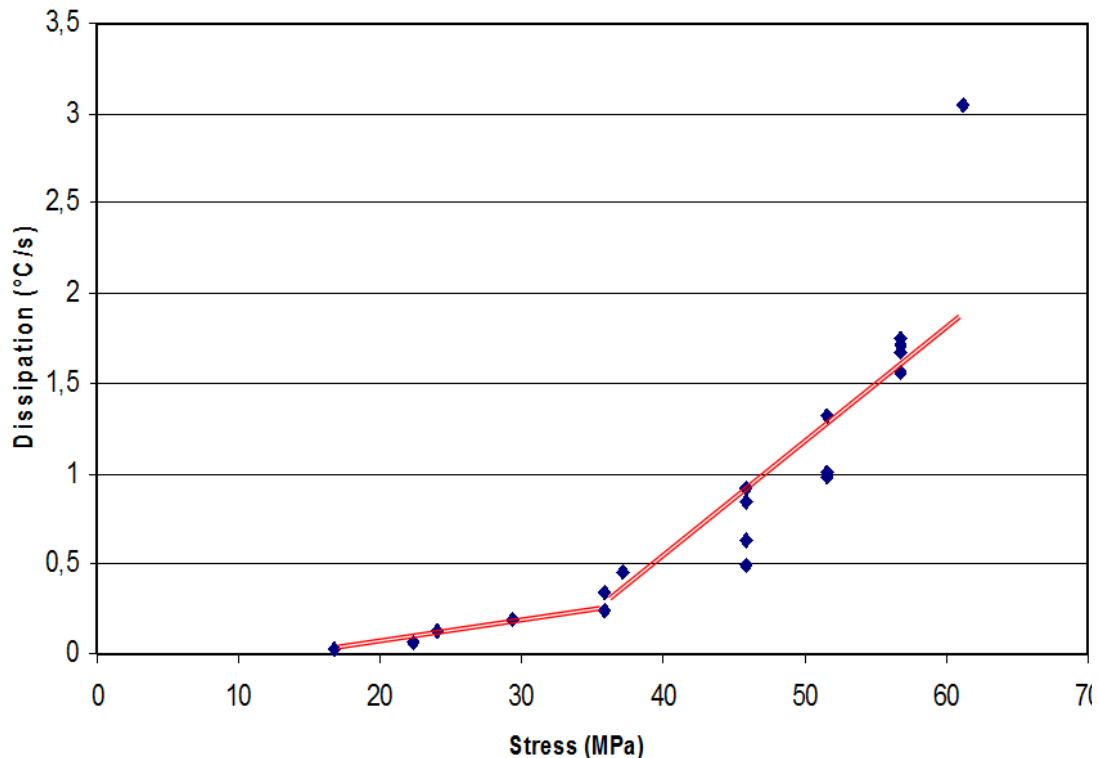


Figure 5. Average intrinsic dissipation at 10^7 cycles vs maximum stress amplitude

4. DISCUSSION

Stanzl-Tschegg et al [2] studied polycrystalline pure copper of mean grain size of about $60 \mu\text{m}$ so quite similar to the material of interest here. The fatigue limit at 1×10^{10} cycles in the VHCF regime reached an ultrasonic system at 20 kHz was found equal to $\Delta\sigma/2 = 92.2 \text{ MPa}$. They defined a PSB threshold associated with the emergence of slip bands at the specimen surface at 2×10^6 cycles. They found $\Delta\sigma/2 = 62.6 \text{ MPa}$ [2]. In the present work, the slip bands were observed at the stress amplitude $\Delta\sigma/2 = 72.1 \text{ MPa}$ which is higher than this PSB threshold. Hence, in this case, slip markings are obviously PSBs with regard to other works [8-9]. Recently, a new PSBs threshold equal to $\Delta\sigma/2 = 45 \text{ MPa}$ was associated with the emergence of slip bands at the specimen surface at 2.7×10^8 cycles [9]. Note that the authors checked the "persistent" nature of the slip bands by electropolishing after fatigue and reloading technique. Transmission electron microscopy (TEM) studies on these slip bands revealed that strongly elongated dislocation cells rather than ladder-like dislocation structure are observed beneath the PSBs. Stanzl-Tschegg et al also suggested the existence of a slip band threshold associated with the appearance of slip marking that are not PSBs. They estimated it equal to 34 MPa at 1.3×10^{10} cycles for which they observed one single slip band of the specimen surface. It is worth noticing that this value is in very good agreement with the

change of dissipative regime mentioned above. For stress amplitude lower than 35 MPa, we found that the dissipation is not null and increase very slowly along cycles. Following previous works [6], we suggest that this dissipation comes from the small amplitude glide of mobile dislocations. This glide is mainly recoverable under cyclic loading and so does not lead to any markings at the specimen surface but dissipate energy. At stress amplitudes higher than 35 MPa, new mobile dislocations are probably created and so more and more dislocations glide leading to an increase of the dissipation along cycles and a higher level of dissipation. Owing to the accumulation of slip irreversibility (unrecoverability), slip markings can appear at the specimen surface. The number of cycles corresponding to the appearance of slip markings clearly decreases with increasing the stress amplitudes.

5. CONCLUSIONS

The internal change of polycrystalline pure copper due to cyclic loading in the VHCF regime was characterized by coupling two methods: (1) observing the specimen surface change during cycling and (2) estimating the intrinsic dissipation from temperature measurements. The main conclusions are the following:

- the material dissipates energy even at stress amplitudes lower than the σ_{slip} band threshold defined by Stanzl-Tschegg et al [2],
- It exists a dissipation threshold associated with a change of dissipation regime. This change of dissipation regime is found equal to the σ_{slip} band threshold
- For stress amplitudes higher than the σ_{slip} band threshold the dissipation is related to the microplasticity activity: higher dissipation corresponds to higher quantity of slip markings.

ACKNOWLEDGMENT: We thank Agence Nationale de la Recherche France ANR-09-BLAN-0025-01 for their financial support and the company Griset for supplying copper.

6. REFERENCES

1. H. Mughrabi, *Int. J. Fat.*, 28, 2006, 1501–1508
2. S. E. Stanzl-Tschegg, H. Mughrabi, B. Schoenbauer, *Int. J. Fat.*, 29, 2007, 2050–2059
3. T. Boulanger, A. Chrysochoos, C. Mabru, A. Galtier, *Int. J. Fat.*, 26, 2004, 221-229
4. C. Doudard, S. Calloch, F. Hild, S. Roux, *Mech Mater.* 42, 2010, 55-62
5. N. Connesson, F. Maquin, F. Pierron, *Exp. Mech.* 51, 2011, 23-44
6. C. Mareau, V. Favier, B. Weber, A. Galtier, *Int. J. Fat.*, 31, 2009, 1407-1412
7. M.P. Luong, *Mech Mater* 28, 1998, 155-163.
8. A. Weidner, C. Blochwitz, W. Skrotzki, W. Tirschler, *Mater. Sci. Eng. A* 479, 2008, 181–190
9. S. E. Stanzl-Tschegg, B. Schönbauer, *Int. J. Fat.*, 32 (2010) 886–893